

Condensate wave function and elementary excitations of bosonic polar molecules: beyond the first Born approximation

Chao-Chun Huang¹, Daw-Wei Wang^{2,3}, and Wen-Chin Wu¹

¹ *Department of Physics, National Taiwan Normal University, Taipei 11650, Taiwan*

² *Physics Department, National Tsing-Hua University, Hsinchu 300, Taiwan*

³ *Physics Division, National Center for Theoretical Sciences, Hsinchu 300, Taiwan*

We investigate the condensate wave function and elementary excitations of strongly interacting bosonic polar molecules in a harmonic trap, treating the scattering amplitude beyond the standard first Born approximation (FBA). By using an appropriate trial wave function in the variational method, effects of the leading order correction beyond the FBA have been investigated and shown to be significantly enhanced when the system is close to the phase boundary of collapse. How such leading order effect of going beyond the FBA can be observed in a realistic experiment is also discussed.

PACS numbers: 03.75.Hh, 32.80.Pj, 03.65.-w

I. INTRODUCTION

In recent years dipolar gases become a fast growing field of theoretical and experimental interests in the studies of ultracold atoms and molecules. Among several dipolar systems, chromium (⁵²Cr) atoms have been successfully realized and studied to great extents [1–6]. The dipolar interaction effects for ⁸⁷Rb atoms as well as ³⁹K atoms are also observed in different groups [7, 8]. Several polar molecule systems such as CO [9], ND₃ [10], RbCs [11], LiCs [12], and CsCl have also been trapped, cooled, and studied [13, 14]. More recently, a high phase-space density gas of polar ⁴⁰K⁸⁷Rb molecules have also been produced [15]. These stimulate great interest in the studies of dipolar systems at low temperatures. In an earlier theoretical work within the first Born approximation (FBA), Yi and You [16] proposed a pseudopotential to study the long-range dipolar interaction. Based on this approximation, which is justified only in the weak dipole moment limit, various theoretical studies of the excitations, collapses, instability, *etc.* of the dipolar BEC system have been carried out in these years [17].

While Yi and You's pseudopotential within FBA is appropriate for a weakly interacting system, it can not be applied for a polar molecule system of strong interaction. Under a strong field, polar molecules can have a large electric dipole moment to make various shape resonances possible. Therefore one needs to include the interaction beyond the FBA in order to have a better understanding on the low energy behavior of these dipolar systems. Recently, one of us has developed an effective many-body theory for bosonic polar molecules in the strong interaction regime that goes beyond the FBA [18]. It is interesting to investigate how the higher order interactions affect the properties of polar molecules. Following [18], our current paper attempts to study the leading order effects beyond the FBA on the condensate profile and elementary excitations of bosonic polar molecules. It will be shown that the effect of the leading-order term is most prominent when the system is approaching the instability

(collapsed state). This is manifested in both the ground-state property and elementary excitations. In particular, at the intermediate trap aspect ratio, $\lambda = \omega_z/\omega_\rho = 5 \sim 6$, the results obtained by the theories within FBA and going beyond FBA have a drastic difference near the collapsed regime. This drastic change indeed allows one to extract quantitatively the effect beyond FBA in a realistic experiment. In the large λ (pancake) and small λ (cigar) limits, on the other hand, the effects beyond the FBA becomes much reduced and may not be easily observed in the experiment.

The paper is organized as follows. In Sec. II, we outline the effective Hamiltonian for studying the low-energy many-body physics of polar molecules. In Sec. III, a trial wave function, called “modified Gaussian” is introduced and used to calculate the ground-state properties of polar molecules beyond the FBA. In Sec. IV, we investigate the elementary excitations (breathing modes) of the system, and provide an scheme to quantitatively extract the effect beyond the FBA in an experiment. Sec. V is a brief conclusion.

II. EFFECTIVE HAMILTONIAN

The effective Hamiltonian, which describes low-energy many-body physics of bosonic polar molecules beyond the FBA, can be given in the following second quantization formalism (for details, see Ref. [18]):

$$H_{\text{eff}} = \sum_{\mathbf{p}} (\varepsilon_{\mathbf{p}} - \mu) \hat{a}_{\mathbf{p}}^\dagger \hat{a}_{\mathbf{p}} + \frac{1}{\Omega} \sum_{\mathbf{p}_1, \mathbf{p}_2} \hat{a}_{\mathbf{p}_1}^\dagger \hat{a}_{\mathbf{p}_2} V_{\text{ext}}(\mathbf{p}_1 - \mathbf{p}_2) + \frac{1}{2\Omega} \sum_{\mathbf{p}_1, \mathbf{p}_2, \mathbf{P}} \hat{a}_{\frac{1}{2}\mathbf{P}+\mathbf{p}_1}^\dagger \hat{a}_{\frac{1}{2}\mathbf{P}-\mathbf{p}_1}^\dagger \hat{a}_{\frac{1}{2}\mathbf{P}-\mathbf{p}_2} \hat{a}_{\frac{1}{2}\mathbf{P}+\mathbf{p}_2} \Gamma(\mathbf{p}_1, \mathbf{p}_2), \quad (1)$$

where $V_{\text{ext}}(\mathbf{p}_1 - \mathbf{p}_2)$ is the Fourier transform of the external trapping potential and Ω is the system volume.

$\Gamma(\mathbf{p}_1, \mathbf{p}_2)$ is the pseudo-potential responsible for the interaction vortex between polar molecules, and can be divided into the following three parts:

$$\Gamma(\mathbf{p}, \mathbf{p}') = \frac{4\pi\hbar^2 a_s}{M} + V_d(\mathbf{p} - \mathbf{p}') - \frac{4\pi\hbar^2}{M} f_\Delta(\mathbf{p}, \mathbf{p}'). \quad (2)$$

The first term in Eq. (2) is from the standard s -wave scattering and the second term is due to the usual FBA with $V_d(\mathbf{q}) = 4\pi D^2(3\cos^2\theta_{qz} - 1)/3$ being the long-range dipole-dipole interaction. Here D is the electric dipole moment and θ_{qz} is the angle between the z -component wavevector and the total wavevector. The third term, f_Δ , is the scattering amplitude including all the results deviated from the known FBA in the second term. In the general situation, the deviated term can be expanded in different angular momentum channels [18],

$$f_\Delta(\mathbf{p}_1, \mathbf{p}_2) \equiv -4\pi \sum_{l,l'} i^{l'-l} \sum_m \Delta a_{ll'}^{(m)} Y_{lm}^*(\hat{p}_1) Y_{l'm}(\hat{p}_2) \quad (3)$$

where $\Delta a_{ll'}^{(m)} \equiv -i^{l'-l}[t_{lm}^{l'm}(0) - t_{Blm}^{l'm}(0)]$ is the difference between a full scattering length and its FBA result. $Y_{lm}(\hat{p})$ is the spherical harmonics defined by the orientation of momentum \mathbf{p} . In Eq. (3), the sum, $\sum_{l,l'}$, has excluded the contribution from a pure s -wave channel ($l = l' = 0$), which has been already included in the first term of Eq. (2). In the limit of a weak external field, the electric dipole moment is also small and each term in Eq. (2) has the following orders of magnitude: $a_s = \mathcal{O}(D^0)$, $V_d = \mathcal{O}(D^2)$, and $\Delta a_{ll'}^{(m)} = \mathcal{O}(D^4)$ [18]. Thus in the low field (*i.e.*, small- D) limit, $f_\Delta(\mathbf{p}, \mathbf{p}')$ term can be safely neglected within the FBA. However, when the external field is strong enough, the effect of $f_\Delta(\mathbf{p}, \mathbf{p}')$ should be taken into account to go beyond the standard FBA. The actual values of $\Delta a_{ll'}^{(m)}$ have to be calculated from a full scattering theory of polar molecules, as shown in Ref. [19–21].

In the present paper, we shall study how these higher order terms, $\Delta a_{ll'}^{(m)}$, can affect the ground state and the elementary excitation property of a bosonic dipolar molecule gas beyond the first Born approximation level. According to the numerical calculation of these scattering amplitude in Refs. [19, 21], we find that $\Delta a_{ll'}^{(m)}$ becomes smaller for larger angular momentum, l or l' . When near the first shape resonance, it is found that although all scattering channels will diverge, but the most dominant contributions are still from $(l, l') = (0, 0)$ (s -wave), and $(0, 2) = (2, 0)$ channels. Divergences on the $(2, 2)$ channels are almost invisible. When away from the shape resonance regime, the scattering amplitude of higher angular momentum channels ($l > 0$) are well described by the first Born approximation, if only the dipole moment is not too large. Therefore, from a practical point of view, we do not need to investigate all the possible values of $\Delta a_{ll'}^{(m)}$, but, on the other hand, we can concentrate on the effect of the lowest non-trivial terms, $\Delta a_{0,2}^{(0)} \neq 0$ and set $\Delta a_{ll'}^{(0)} = 0$ for all (l, l') not equal to $(0, 2)$, $(2, 0)$, or $(0, 0)$.

As mentioned above, this special case becomes relevant when the electric dipole moment is close to the first shape resonance peak, where the coupling between s -wave and d -wave channels are significantly enhanced. The effect of shape resonance on the s -wave channel, a_s , is also significant, but has been separated in Eq. (2). When the dipole moment is even larger, it is reasonable to expect that more scattering channels will have scattering amplitude different from the first Born approximation result, *i.e.* $\Delta a_{ll'}^{(m)} \neq 0$. However, since it is very difficult to investigate a general properties of such strong interacting limit, here we will still concentrate on the effects beyond the FBA only through the channel, $\Delta a_{0,2}^{(0)} \neq 0$, which will be a good approximation when the external field is near the regime of the first shape resonance [19]. Nevertheless, the effect of next leading term, $\Delta a_{2,2}^{(0)}$, will be briefly studied in Sec. IV.

To calculate the expectation value of the effective Hamiltonian Eq. (1), $E = \langle H_{\text{eff}} \rangle$, one can replace $\hat{a}_{\mathbf{k}}$ by a macroscopic condensate wave function, $\Psi_{\mathbf{k}} \equiv \langle \hat{a}_{\mathbf{k}} \rangle = \frac{1}{\sqrt{\Omega}} \int d\mathbf{r} \Psi(\mathbf{r}) e^{-i\mathbf{k} \cdot \mathbf{r}}$ in (1) at zero temperature. We can then apply the variational method to obtain the ground-state energy of the system. If one uses the (normalized) simple Gaussian-type trial wave function ($\rho^2 = x^2 + y^2$),

$$\Psi(\mathbf{r}) = \frac{\exp(-\rho^2/2R_0^2 - z^2/2R_z^2)}{\pi^{3/4} R_0 R_z^{1/2}}, \quad (4)$$

with R_0 and R_z the Gaussian radii of the condensate in the x - y plane and along the z axis respectively and assumes that the harmonic trapping potential is $V_{\text{ext}}(\mathbf{r}) = \frac{1}{2}m\omega_\rho^2\rho^2 + \frac{1}{2}m\omega_z^2z^2$ with ω_ρ and ω_z the trapping frequencies, variational energy of Eq. (1) becomes (see also Eq. (16) of [18])

$$\frac{E(R_0, R_z)}{E_0} = E_k + E_{\text{trap}} + E_{\text{int}}, \quad (5)$$

where

$$E_k = \frac{R_0^2 + 2R_z^2}{4R_z^2 R_0^2}, \quad (6)$$

$$E_{\text{trap}} = \frac{2R_0^2 + \lambda^2 R_z^2}{4}, \quad (7)$$

and

$$E_{\text{int}} = \frac{N}{\sqrt{2\pi}R_0^3} \left[a_s \frac{R_0}{R_z} + 8 \left(\frac{a_d}{3\sqrt{5}} - \Delta a_{0,2}^{(0)} \right) A_2 \left(\frac{R_0}{R_z} \right) \right] \quad (8)$$

correspond to the kinetic energy, trapping potential energy, and interaction energy respectively. Note that the above results include only the leading higher-order term, $\Delta a_{0,2}^{(0)}$. Here $A_l(\frac{R_0}{R_z}) \equiv \frac{\sqrt{2l+1}}{8} \int_{-1}^1 dx \frac{P_l(x)}{(1 + ((R_0/R_z)^2 - 1)x^2)^{3/2}}$ and $\lambda \equiv \omega_z/\omega_\rho$ is the trapping aspect ratio. All lengths, a_s , $a_d \equiv MD^2/\hbar^2$, $\Delta a_{0,2}^{(0)}$, R_0 , and R_z , are scaled by the harmonic oscillator length, $a_{\text{osc},0} \equiv \sqrt{\hbar/M\omega_\rho}$. $E_0 \equiv N\hbar^2/ma_{\text{osc},0}^2$ is the energy scale. Throughout this paper, we will use the same length and energy scales.

It is convenient to redefine: $\zeta_s \equiv Na_s, \zeta_d \equiv Na_d$, and $\zeta_{0,2} \equiv -3\sqrt{5}N\Delta a_{0,2}^{(0)}$ such that the interaction term Eq. (8) can be rewritten as

$$E_{\text{int}} = \frac{1}{\sqrt{2\pi}R_0^3} \left[\zeta_s \frac{R_0}{R_z} + \frac{8}{3\sqrt{5}}(\zeta_d + \zeta_{0,2})A_2\left(\frac{R_0}{R_z}\right) \right]. \quad (9)$$

In view of Eq. (9) or (8), it poses a subtlety that both the dipolar interaction ζ_d and the higher-order interaction $\zeta_{0,2}$ couple to the same function. This result is just an artifact of the Gaussian trial wave function and should not exist in a more general condensate wave function as stated in Ref. [18].

III. BEYOND THE FBA: GROUND-STATE PROPERTY

In order to separate the contribution of the $\Delta a_{0,2}^{(0)}$ for the usual FBA result, in this paper we use the following “modified Gaussian” (MG) trial wave function

$$\Psi(\mathbf{r}) = C \exp(-\rho^2/2R_0^2 - z^2/2R_z^2) \times \left(1 + \frac{a_0\rho^2}{R_0^2} + \frac{a_z z^2}{R_z^2} \right), \quad (10)$$

where R_0, R_z, a_0 , and a_z are variational parameters and $C = 2\pi^{-3/4}/[R_0\sqrt{R_z}(8a_0^2 + 4a_0a_z + 3a_z^2 + 8a_0 + 4a_z + 4)]$ is the normalization factor. Function (10) can be viewed as the simple Gaussian (SG) multiplied (modified) by a parabolic function. In Ref. [22], a similar MG trial function (SG function multiplied by a hypercosine function) was first introduced and used to study one- and two-component ultracold BEC systems. When the MG trial wave function, Eq. (10), is used to calculate the energy functional, $E = E(R_0, R_z, a_0, a_z)$, ground-state energy of the system can be obtained by minimizing E . That is, it requires that $\partial E/\partial \beta_i = 0$ are satisfied for all four variational parameter $\beta_i = R_0, R_z, a_0, a_z$. Comparison between the results due to a SG and a MG trial wave function for one- and two-component ultracold BEC systems without a dipolar interaction can be found in Ref. [22].

To justify the appropriateness of MG trial wave function (10) in the variational studies of strong dipolar BEC systems, we refer to the following. Recent numerical studies on dipolar BEC systems have revealed structured ground-state density profiles in them [23, 24]. Of most interest, density profile can exhibit a double-peak structure, so-called “biconcave condensates”, for dipolar BECs. In a recent work of Jiang and Su [25], it has been shown that the structured double-peak ground state density profile can be successfully reproduced in the variational approach based on a similar trial wave function, analogous to (10). Thus it is believed that, at least in the qualitative manner, MG trial wave function should be a good one for studying the higher-order effect beyond the FBA in strongly interacting dipolar BEC systems. It is hoped that a more accurate numerical approach, which is difficult but is underway, can be completed soon.

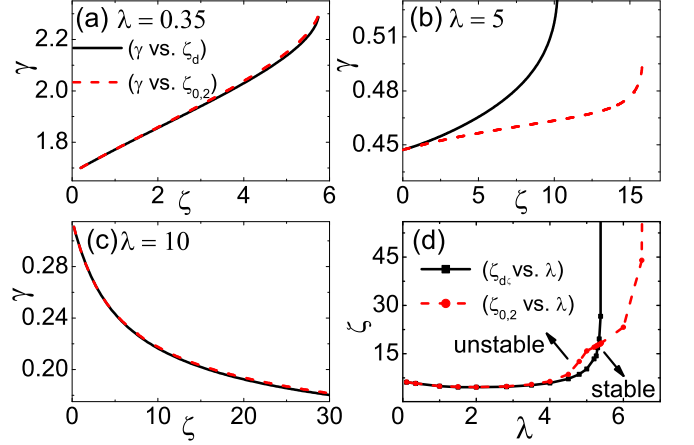


FIG. 1. (Color online) In frame (a)-(c), the condensate aspect ratio, γ (see text for the definition), is plotted for MG against the value of dimensionless ζ_d ($\zeta_{0,2}$ set to zero) or $\zeta_{0,2}$ (ζ_d set to zero) for three trapping aspect ratio $\lambda = \omega_z/\omega_\rho = 0.35, 5$ and 10 . Frame (d) shows the phase boundary separating the unstable (collapsed) state from the stable state. In all frames, $\zeta_s = 0$ is taken.

When the MG (10) is used as the trial wave function, the three terms of the variational energy become

$$E_k = \frac{R_0^2 + 2R_z^2}{4R_z^2 R_0^2} - B \left(\frac{4a_0}{R_0^2} + \frac{2a_z}{R_z^2} - \frac{a_z^2}{R_z^2} + 2a_0a_z \frac{R_0^2 + R_z^2}{R_z^2 R_0^2} \right),$$

$$E_{\text{trap}} = \frac{1}{B} [R_0^2(2 + 8a_0 + 2a_z + 12a_0^2 + 3a_z^2 + 4a_0a_z) + R_z^2\lambda^2(1 + 2a_0 + 3a_z + 2a_0^2 + 15a_z^2 + 3a_0a_z)],$$

and

$$E_{\text{int}} = \zeta_s A_s(a_0, a_z, R_0, R_z) + \zeta_d A_d(a_0, a_z, R_0, R_z) + \zeta_{0,2} A_{0,2}(a_0, a_z, R_0, R_z), \quad (11)$$

where $B = (4a_z + 8a_0^2 + 3a_z^2 + 8a_0 + 4a_0a_z + 4)$. A_s, A_d , and $A_{0,2}$ are lengthy functions of a_0, a_z, R_0 , and R_z whose explicit forms are given in Appendix A. One can simply check that when $a_0 = a_z = 0$, $B \rightarrow 4$ and E_k and E_{trap} reduce to those for the SG case [see Eqs. (6) and (7)]. E_{int} will also reduce to that for the SG case (see Appendix A).

As seen clearly in E_{int} in Eq. (11), $\zeta_d A_d$ and $\zeta_{0,2} A_{0,2}$ correspond to the contributions of dipolar interaction and higher order $\Delta a_{0,2}^{(0)}$ interaction to the ground-state energy. Thus the regime at which the two terms become most distinct is also the regime to see the effect beyond the FBA most clearly. In this section, we will investigate such beyond-FBA effect from the condensate aspect ratio, γ , which is defined as

$$\gamma \equiv \sqrt{I_z/I_x}, \quad (12)$$

where

$$I_z = \int |\Psi(\mathbf{r})|^2 z^2 d\mathbf{r}$$

$$I_x = \int |\Psi(\mathbf{r})|^2 x^2 d\mathbf{r} = \int |\Psi(\mathbf{r})|^2 y^2 d\mathbf{r}. \quad (13)$$

In Fig. 1(a)–(c), based on the MG trial wave function, we show results of the ground-state aspect ratio, γ , against the dipolar interaction strength, ζ_d , for $\zeta_{0,2} = 0$, and against $\zeta_{0,2}$ by setting $\zeta_d = 0$ for three different values of the trapping aspect ratio, λ . Note that, although such kind of interaction is not realistic in the experiment, but it provides a direct evidence to distinguish the effects of dipolar interaction in the FBA and beyond the FBA. In view of Fig. 1(a) and (c), for the $\lambda = 0.35$ and 10 cases, the effects of ζ_d and $\zeta_{0,2}$ are almost the same within the parameter regime we calculate, because the condensate aspect ratio is mostly determined by the trapping aspect ratio directly, i.e. the interaction effect is negligible. In contrast, for the case of $\lambda = 5$ [see Fig. 1(b)], the effects of ζ_d and $\zeta_{0,2}$ are quite distinct: the system becomes collapsed more easily for the case of a pure FBA interaction, ζ_d (solid line), while it becomes less easily collapsed for the other case (dashed line). In Fig. 1(d), we show the critical value of ζ for these two cases as a function of the trapping aspect ratio, λ . One sees that system becomes always stable when λ is larger than 5.3 for the bare FBA result, while it requires 6.5 for a pure $\Delta a_{0,2}^{(0)}$, the leading order effect beyond the FBA. Our result indicates that $\zeta_{0,2}$ acts more attractively than ζ_d in the intermediate λ regime.

It is useful to note that regarding where the system collapses, there might be some quantitative difference between the variational and numerical results. Under the condition of same λ , real system could collapse more easily than what the variational theory predicts in the smaller dipolar interaction regime [23, 26]. In addition, for large λ (the system is of pancake shape), the system could also be unstable at large ζ_d [23, 24]. Nevertheless, we emphasize that the qualitative features predicted by the variational method should still be reliable for large ζ_d so long as λ is not too large. The latter is exactly what is studied in the current context.

IV. BEYOND THE FBA: ELEMENTARY EXCITATIONS

This section devotes to the elementary excitations of a dipolar condensate beyond the first Born approximation. As sketched in Fig. 2, two types of collective modes, namely the in-phase and out-of-phase breathing modes, are considered here. They are of particular importance because they are the lowest two excitation modes in a trapped condensate [26, 27]. In the paper of G3ral and Santos [17], these two modes were also called breathing and quadrupole modes. For simplicity of presentation, we will show the results only for the lower-energy one,

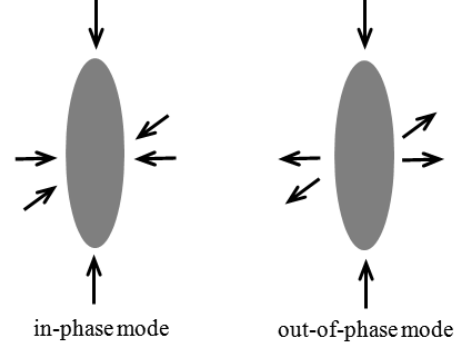


FIG. 2. Schematic plot of the in-phase and out-of-phase breathing modes of an anisotropic dipolar gas. In Ref. [17], these two kinds of modes are called breathing and quadrupole modes.

although both of them are simultaneously obtained in the same method.

In this paper, variational method is applied to study the collective excitation of a system. It corresponds to solving the stationary point of the action $S = \int dt L$, where the Lagrangian $L = T - E$ with $T = \int d\mathbf{r} (i\hbar/2) [\Psi^*(\mathbf{r}) \partial \Psi(\mathbf{r}) / \partial t - \Psi(\mathbf{r}) \partial \Psi^*(\mathbf{r}) / \partial t]$ and E is obtained by the sum of the terms in Eq. (11). For the study of breathing modes, the MG trial function in Eq. (10) will be generalized to include dynamical variables as follows:

$$\Psi(\mathbf{r}, t) = C(t) e^{\left[-\frac{\rho^2(1+\varepsilon_0(t)+i\varepsilon'_0(t))}{2R_0^2} - \frac{z^2(1+\varepsilon_z(t)+i\varepsilon'_z(t))}{2R_z^2} \right]}$$

$$\times \left(1 + \frac{a_0(1+\varepsilon_0(t))\rho^2}{R_0^2} + \frac{a_z(1+\varepsilon_z(t))z^2}{R_z^2} \right). \quad (14)$$

Here, in a cylindrically symmetric trap, ε_i and ε'_i ($i = 0, z$) correspond to the fluctuations of local amplitude and local phase of the dipole cloud associated with the ρ and z directions. As mentioned before, the values of R_0 , R_z , a_0 , and a_z are determined by minimizing the energy functional. After some lengthy derivations, we obtain the dispersions for the breathing modes:

$$\omega^2 = \{f_1 f_4 + f_2 f_5 \pm [(f_1 f_4 - f_2 f_5)^2 + 4f_3^2 f_4 f_5]^{1/2}\} / 2, \quad (15)$$

where \pm correspond to the in-phase or out-of-phase modes and

$$f_1 = \frac{1}{2} \frac{\partial^2 E}{\partial R_0^2}, \quad f_2 = \frac{1}{2} \frac{\partial^2 E}{\partial R_z^2}, \quad f_3 = \frac{\partial^2 E}{\partial R_z \partial R_0}, \quad (16)$$

$$f_4 = B(4 + 16a_0 + 4a_z + 24a_0^2 + 3a_z^2 + 8a_0 a_z)^{-1},$$

$$f_5 = 2B(4 + 8a_0 + 12a_z + 8a_0^2 + 15a_z^2 + 12a_0 a_z)^{-1}.$$

To determine which one corresponds to the in-phase or out-of-phase mode in (15) requires solving explicitly the time dependence of the dynamical variables.

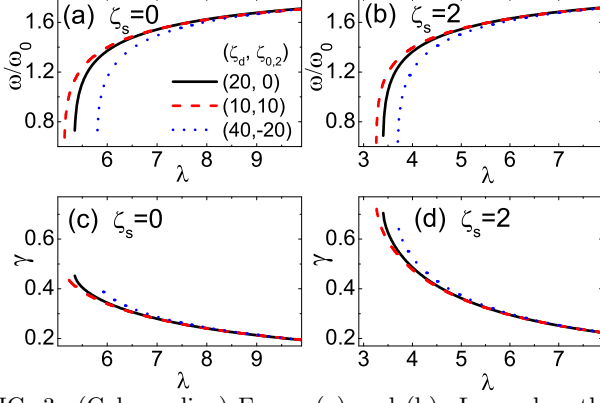


FIG. 3. (Color online) Frame (a) and (b): Lower breathing mode frequencies are plotted as a function of λ for three combinations, $(\zeta_d, \zeta_{0,2}) = (10, 10), (20, 0)$, and $(40, -20)$. Here $\zeta_s = 0$ for (a) and $\zeta_s = 2$ for (b). Frame (c) and (d): Parallel to frame (a) and (b), γ ratios are plotted as a function of λ .

In the following, a case study is given first, which will lead to an explicit idea how to extract quantitatively the $\zeta_{0,2}$ term in real experiments. In ^{52}Cr atom dipolar BEC, it was measured that $D^2M/\hbar^2 \simeq 24 \text{ \AA}$. If atom number is about $N = 10^4$ and the harmonic oscillator length is about $1\mu\text{m}$, ζ_d will be about 20. For polar molecule systems, ζ_d could be 100 times larger than that of ^{52}Cr atom dipolar BEC [27]. Nevertheless, here we study the case of $\zeta_d + \zeta_{0,2} = 20$ to which three combinations of $(\zeta_d, \zeta_{0,2}) = (10, 10), (20, 0)$, and $(40, -20)$ are considered.

In Fig. 3(a) and (b), the lower breathing modes for these three combinations are presented and compared as a function of trapping aspect ratio λ . In the current context, the lower breathing mode oscillates out-of-phase. This is mainly due to the fact that s -wave interaction is relatively small and the dipolar interaction dominates. Since dipolar interaction is anisotropic: attractive along the z direction while repulsive in the xy plane, consequently out-of-phase mode has lower energy than that of the in-phase mode. Fig. 3(a) corresponds to the case of $\zeta_s = 0$. In view of Fig. 3(a), two important features are revealed: (i) all three curves merge in the large λ limit (i.e. a pancake like trapping potential) and (ii) the curves deviate each other significantly when the system is close to the phase boundary of collapse. For instances when $\lambda = 5.9$, $\omega = 1.338\omega_0$ for the case $(\zeta_d, \zeta_{0,2}) = (20, 0)$, while $\omega = 1.044\omega_0$ for the case $(\zeta_d, \zeta_{0,2}) = (40, -20)$. The relative frequency difference, $\Delta\omega \equiv |\omega_1 - \omega_2|/\omega_2$, can be 21% large. $\Delta\omega$ will increase even more significantly when the system is approaching the collapsed regime. Similar behaviors are also found in Fig. 3(b), where a finite value of s -wave scattering length is included ($\zeta_s = 2$).

In Fig. 3(c) and (d), we show the condensate aspect ratio, γ , as a function of λ . In view of Fig. 3(c) with $\zeta_s = 0$, one finds that all three γ curves also merge in the large λ limit. Besides, when $\lambda = 5.9$ close to the collapsed regime, $\gamma = 0.353$ and 0.392 respectively for the case of $(\zeta_d, \zeta_{0,2}) = (20, 0)$ and $(40, -20)$. The relative γ

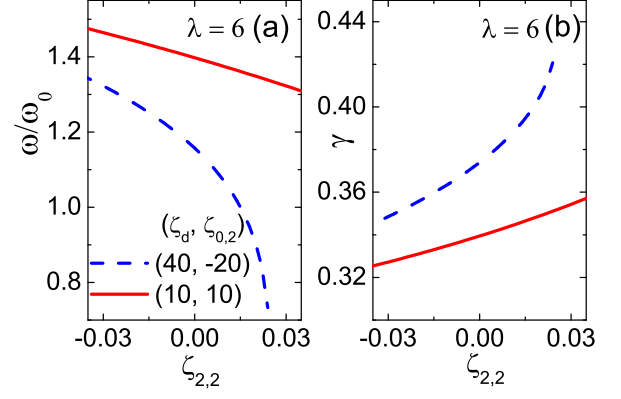


FIG. 4. (Color online) (a) Lower breathing mode and (b) γ ratio of the dipolar system are plotted as a function of $\zeta_{2,2}$. In both frames, $\lambda = 6$ and two combinations of $(\zeta_d, \zeta_{0,2}) = (10, 10)$ and $(40, -20)$ are chosen. Here we set $\zeta_s = 0$.

difference, $\Delta\gamma \equiv |\gamma_1 - \gamma_2|/\gamma_2$, is about 11%. In Fig. 3(d) with $\zeta_s = 2$, when $\lambda = 3.8$, γ ratio is 0.528 and 0.593 for the case of $(\zeta_d, \zeta_{0,2}) = (20, 0)$ and $(40, -20)$. This gives a relatively smaller $\Delta\gamma = 2\%$. Similar to the $\Delta\omega$ case, $\Delta\gamma$ will increase significantly when the system is even more close to the collapsed regime.

It should be emphasized that in the case that ζ_s is large or the sum of $\zeta_d + \zeta_{0,2}$ is small, the system will tend to stabilize over a large span of λ . This means that whatever combinations of ζ_d and $\zeta_{0,2}$ under $\zeta_d + \zeta_{0,2} = \text{const}$ will roughly lead to the same curve. Thus, $\Delta\omega$ or $\Delta\gamma$ studied above, will always be small, i.e. the effect of the effects beyond the FBA cannot be observed easily.

In the following, we propose how to extract quantitatively the value of $\zeta_{0,2}$ by measuring the lower breathing mode frequency or the condensate aspect ratio γ of the system. Firstly, we assume that the value of ζ_s is relatively small such that the behaviors of breathing mode frequency and γ ratio resemble those in Fig. 3(a)-(d). Suppose that one does not know the value of any one of ζ_s , ζ_d , and $\zeta_{0,2}$. One can first perform the measurement of the lower breathing mode frequency and/or γ ratio at large λ case, say $\lambda = 10$. As shown in Fig. 3(a)-(d), all three curves merge at large λ limit. This means that one can unambiguously determine the values of both ζ_s and the sum of ζ_d and $\zeta_{0,2}$ simply by carrying out a theoretical fitting to the experimental data. The next task is to separate the values of ζ_d and $\zeta_{0,2}$. For this purpose, one can redo the experiment and decrease λ to approach the collapsed regime. Since at this regime, the fitting will be quite sensitive to both values of ζ_d and $\zeta_{0,2}$, one can then unambiguously determine the value of $\zeta_{0,2}$ by comparing with our theoretical calculation result.

Now we provide a short discussion on the effect of the next order effect beyond the FBA by including finite value of $\Delta a_{2,2}^{(0)}$. Same as before, we define $\zeta_{2,2} \equiv N\Delta a_{2,2}^{(0)}$ for the convenience. In Fig. 4 we show the lower breath-

ing mode frequency and the aspect ratio, γ , as a function of $\zeta_{2,2}$ for a fixed trapping aspect ratio, $\lambda = 6$. Two combinations of $(\zeta_d, \zeta_{0,2}) = (10, 10)$ and $(40, -20)$ are chosen and it is assumed that $\zeta_s = 0$. As $\zeta_{2,2}$ increases, it is found that the system becomes more cigar-like shape (i.e. γ becomes larger), while it becomes more pancake-like shape when $\zeta_{2,2}$ is negative. Positive $\zeta_{2,2}$ will lead the system to be more attractive along the z direction and hence more easily collapsed. However its effect is relatively weaker compared to that of the $\zeta_{0,2}$ term discussed before.

V. CONCLUSION

This paper attempts to study the ground state and elementary excitations of a strongly interacting dipolar bosonic gas based on a theory going beyond the first Born approximation (FBA). By using an appropriate trial wave function in the variational method, the leading higher-order corrections to the FBA are studied in details, in particular for the condensate aspect ratio and the elementary excitation mode frequency. Of most interest, it is found that the effect of the corrections is most important when the system is close to phase boundary of collapse. Through several case studies with parameters pertaining to ^{52}Cr atom dipolar BEC, it is believed that the higher-order effect going beyond FBA should be even more significant and highly observable in the strong dipolar molecule system. An idea for extracting quantitatively such leading-order effect beyond the FBA in real experiments is provided. Finally, to shed more light on understanding the higher-order effect, a more accurate numerical calculation is in demand.

ACKNOWLEDGMENTS

We are grateful to the support of National Science Council and National Center for Theoretical Sciences, Taiwan.

Appendix A: Forms of Functions A

In this Appendix, we give explicit forms of functions A_s , A_d , and $A_{0,2}$ appearing in Eq. (11). Function A_s is analytic and given by

$$A_s = \frac{\sqrt{2}}{\sqrt{\pi} R_z R_0^2 (8 a_0^2 + 4 a_z a_0 + 8 a_0 + 4 a_z + 3 a_z^2 + 4)^2} \times \left[12 a_0^4 + (24 + 6 a_z) a_0^3 + \left(24 + 12 a_z + \frac{9}{2} a_z^2 \right) a_0^2 + \left(16 + 12 a_z + 9 a_z^2 + \frac{15}{4} a_z^3 \right) a_0 \right]$$

$$+ \frac{105}{32} a_z^4 + \frac{15}{2} a_z^3 + 9 a_z^2 + 8 a_z + 8 \Big]. \quad (\text{A1})$$

Functions A_d and $A_{0,2}$ are represented by an integral in the cylindrical coordinate, (k_r, k_φ, k_z) . More precisely A_d is given by

$$A_d = \int_{-\infty}^{\infty} dk_z \int_0^{\infty} 2\pi k_r dk_r \eta_d \quad (\text{A2})$$

with

$$\eta_d = \frac{e^{-(R_z^2 k_z^2 + R_0^2 k_r^2)/2} (3 k_z^2 / (k_r^2 + k_z^2) - 1)}{12\pi^2 (4 a_0 a_z + 8 a_0 + 8 a_0^2 + 4 + 4 a_z + 3 a_z^2)^2} \times \left[4 a_0 a_z + 8 a_0 + 8 a_0^2 + 4 + 4 a_z + 3 a_z^2 - (2 a_0 + 2 + 3 a_z) a_z R_z^2 k_z^2 - (2 + 4 a_0 + a_z) a_0 R_0^2 k_r^2 + \frac{a_z^2 R_z^4 k_z^4}{4} + \frac{a_0^2 R_0^4 k_r^4}{4} + \frac{a_0 a_z R_0^2 R_z^2 k_z^2 k_r^2}{2} \right]^2, \quad (\text{A3})$$

while $A_{0,2}$ is given by

$$A_{0,2} = \int_{-\infty}^{\infty} dk_z \int_0^{\infty} 2\pi k_r dk_r \eta_{0,2} \quad (\text{A4})$$

with

$$\eta_{0,2} = \frac{e^{-(R_z^2 k_z^2 - R_0^2 k_r^2)/2} (3 k_z^2 / (k_r^2 + k_z^2) - 1)}{12\pi^2 (4 a_0 a_z + 8 a_0 + 8 a_0^2 + 4 + 4 a_z + 3 a_z^2)^2} \times \left[C_{rz} a_0 a_z R_0^2 R_z^2 k_r^2 k_z^2 + D_r a_0^2 R_0^4 k_r^4 + D_z a_z^2 R_z^4 k_z^4 + C_0 + C_r a_0 R_0^2 k_r^2 + C_z a_z R_z^2 k_z^2 \right]. \quad (\text{A5})$$

Here C_0 , C_r , C_z , C_{rz} , D_r , and D_z are given as follows:

$$\begin{aligned} C_0 &= 40 a_0^4 + (44 a_z + 96) a_0^3 + (33 a_z^2 + 96 a_z + 112) a_0^2 \\ &\quad + \left(\frac{39}{2} a_z^3 + 60 a_z^2 + 88 a_z + 64 \right) a_0 \\ &\quad + \frac{81}{16} a_z^4 + 18 a_z^3 + 34 a_z^2 + 32 a_z + 16, \\ C_r &= - \left(\frac{21}{4} a_z^3 + 11 a_0 a_z^2 + 13 a_z^2 + 14 a_0^2 a_z + 32 a_0 a_z \right. \\ &\quad \left. + 20 a_z + 40 a_0^2 + 48 a_0 + 16 + 16 a_0^3 \right), \\ C_z &= - \left(\frac{3}{4} a_z^3 + 9 a_z^2 + \frac{15}{2} a_0 a_z^2 + 18 a_0^2 a_z + 28 a_z \right. \\ &\quad \left. + 36 a_0 a_z + 20 a_0^3 + 40 a_0^2 + 40 a_0 + 16 \right), \\ C_{rz} &= \left(\frac{3}{2} a_z^2 + 4 a_z + 2 a_0 a_z + 8 + 8 a_0 + 4 a_0^2 \right), \\ D_r &= \left(\frac{3}{4} a_z^2 + 2 a_z + a_0 a_z + 4 + 4 a_0 + 2 a_0^2 \right), \\ D_z &= \left(\frac{3}{4} a_z^2 + 2 a_z + a_0 a_z + 4 + 4 a_0 + 2 a_0^2 \right). \quad (\text{A6}) \end{aligned}$$

When $a_0 = a_z = 0$, the two integrals for A_d and $A_{0,2}$ become equal.

-
- [1] A. Griesmaier, J. Werner, S. Hensler, J. Stuhler and T. Pfau, Phys. Rev. Lett. **94**, 160401 (2005).
 - [2] J. Stuhler, A. Griesmaier, T. Koch, M. Fattori, T. Pfau and S. Giovanazzi, P. Pedri, L. Santos, Phys. Rev. Lett. **95**, 150406 (2005).
 - [3] M. Fattori, T. Koch, S. Giotz, A. Griesmaier, S. Hensler, J. Stuhler, and T. Pfau, Nature Phys. **2**, 765 (2006).
 - [4] A. Griesmaier, J. Stuhler, T. Koch, M. Fattori, T. Pfau and S. Giovanazzi, Phys. Rev. Lett. **97**, 250402 (2006).
 - [5] T. Lahaye, T. Koch, B. Fröhlich, M. Fattori, J. Metz, A. Griesmaier, S. Giovanazzi, and T. Pfau, Nature **448**, 672 (2007).
 - [6] T. Koch, T. Lahaye, J. Metz, B. Fröhlich, A. Griesmaier, and T. Pfau, Nature Physics **4**, 218 (2008).
 - [7] M. Vengalattore, S. R. Leslie, J. Guzman, and D. M. Stamper-Kurn, Phys. Rev. Lett. **100**, 170403 (2008).
 - [8] M. Fattori, C. D'Errico, G. Roati, M. Zaccanti, M. Jonas-Lasinio, M. Modugno, M. Inguscio, and G. Modugno, Phys. Rev. Lett. **100**, 080405 (2008).
 - [9] J.M. Doyle, B. Friedrich, Nature **401**, 749 (1999).
 - [10] H.L. Bethlem, G. Berden, F.M.H. Crompvoets, R.T. Jongma, A.J.A. van Roij, G. Meijer, Nature **406**, 491 (2000).
 - [11] J.M. Sage, S. Sainis, T. Bergeman, D. DeMille, Phys. Rev. Lett. **94**, 203001 (2005).
 - [12] J. Deiglmayr et al., Phys. Rev. Lett. **101**, 133004 (2008).
 - [13] J. Doyle, B. Friedrich, R.V. Krems, F. Masnou-Seeuws, Eur. Phys. J. D **31**, 149 (2004).
 - [14] D. Egorov, W.C. Campbell, B. Friedrich, S.E. Maxwell, E. Tsikata, L.D. van Buuren, J.M. Doyle, Eur. Phys. J. D **31**, 307 (2004).
 - [15] K.-K. Ni, *et al.*, Science **322**, 231 (2008).
 - [16] S. Yi and L. You, Phys. Rev. A **61**, 041604 (2000).
 - [17] K. Góral and L. Santos, Phys. Rev. A **66**, 023613 (2002).
 - [18] D.W. Wang, N. J. Phys. **10**, 053005 (2008).
 - [19] B. Deb and L. You, Phys. Rev. A **64**, 022717 (2001).
 - [20] D.C.E. Bortolotti *et al.*, Phys. Rev. Lett. **97** 160402 (2007); S. Ronen, *et al.*, Phys. Rev. A **74** 033611 (2006); K. Kanjilal, J.L. Bohn, and D. Blume, Phys. Rev. A **75**, 052703 (2007).
 - [21] K. Kanjilal and D. Blume, Phys. Rev. A **78**, 040703 (2008).
 - [22] C.C. Huang and W.C. Wu, Phys. Rev. A **75**, 023609 (2007).
 - [23] Shai Ronen, Daniele C. E. Bortolotti, and John L. Bohn, Phys. Rev. Lett. **98**, 030406 (2007).
 - [24] O. Dutta and P. Meystre, Phys. Rev. A **75**, 053604 (2007).
 - [25] T. F. Jiang and W. C. Su, Phys. Rev. A **74**, 063602 (2006).
 - [26] S. Ronen, D.C.E. Bortolotti and J.L. Bohn, Phys. Rev. A **74**, 013623 (2006).
 - [27] M.A. Baranov, Phys. Rep. **464**, 71 (2008).